

Daniël C. de Geus,* Ellen A. J. Thomassen, Clarisse L. van der Feltz and Jan Pieter Abrahams

Biophysical Structural Chemistry, Leiden University, Einsteinweg 55, 2333 CC Leiden, The Netherlands

Correspondence e-mail:
 d.de.geus@chem.leidenuniv.nl

Received 19 June 2008
 Accepted 3 July 2008

Cloning, expression, purification, crystallization and preliminary X-ray diffraction analysis of chlorite dismutase: a detoxifying enzyme producing molecular oxygen

Chlorite dismutase, a homotetrameric haem-based protein, is one of the key enzymes of (per)chlorate-reducing bacteria. It is highly active ($>2 \text{ kU mg}^{-1}$) in reducing the toxic compound chlorite to the innocuous chloride anion and molecular oxygen. Chlorite itself is produced as the intermediate product of (per)chlorate reduction. The chlorite dismutase gene in *Azospira oryzae* strain GR-1 employing degenerate primers has been identified and the active enzyme was subsequently overexpressed in *Escherichia coli*. Chlorite dismutase was purified, proven to be active and crystallized using sitting drops with PEG 2000 MME, KSCN and ammonium sulfate as precipitants. The crystals belonged to space group $P2_12_12$ and were most likely to contain six subunits in the asymmetric unit. The refined unit-cell parameters were $a = 164.46$, $b = 169.34$, $c = 60.79 \text{ \AA}$. The crystals diffracted X-rays to 2.1 \AA resolution on a synchrotron-radiation source and a three-wavelength MAD data set has been collected. Determination of the chlorite dismutase structure will provide insights into the active site of the enzyme, for which no structures are currently available.

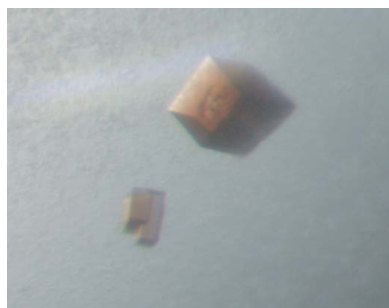
1. Introduction

Azospira oryzae strain GR-1 (DSM 11199) is one of the first perchlorate-reducing bacteria to be described (Rikken *et al.*, 1996; Wolterink *et al.*, 2005). The key enzymes of the dissimilatory (per)chlorate-reducing pathway, (per)chlorate reductase and chlorite dismutase (Cld), were originally purified and characterized from this organism (Kengen *et al.*, 1999; van Ginkel *et al.*, 1996). In addition to perchlorate (ClO_4^-) and chlorate (ClO_3^-), it can utilize O_2 , NO_3^- and Mn^{IV} as electron acceptors, while using various carbon compounds, *e.g.* fatty acids and dicarboxylic acids, or hydrogen as the electron donor (Rikken *et al.*, 1996).

Complete reduction of ClO_4^- into Cl^- and O_2 occurs in several steps. ClO_4^- is reduced to ClO_3^- by a (per)chlorate reductase (EC 1.97.1.1). Subsequently, the same enzyme catalyzes the reduction of ClO_3^- to ClO_2^- . The (per)chlorate reductase has a molecular weight of 420 kDa, with subunits of 95 and 40 kDa (in an $\alpha_3\beta_3$ composition), and contains one [3Fe–4S] cluster, two [4Fe–4S] clusters and one molybdenum cofactor per heterodimer. Although many denitrifying bacteria can reduce ClO_3^- to ClO_2^- , the latter compound is toxic to these cells (Kengen *et al.*, 1999).

(Per)chlorate respiration is made possible by the action of yet another enzyme, chlorite dismutase (EC 1.13.11.49), which reduces the toxic ClO_2^- to environmentally innocuous Cl^- while producing O_2 . Cld is a homotetrameric protein that contains one iron protohaem IX per 30 kDa subunit (Hagedoorn *et al.*, 2002; van Ginkel *et al.*, 1996). Iron-protoporphyrin IX or haem is a ubiquitous enzyme cofactor in nature and haem-based proteins are known to catalyze a wide range of biologically important reactions in all kingdoms of life (Hou *et al.*, 2000; Wilson & Reeder, 2008). However, knowledge of the biochemistry of the (per)chlorate-reductive pathway is still limited.

Determination of the structure of Cld may offer insights into the mechanism of the final step of (per)chlorate reduction. We anticipate that the structural analysis will also open up new routes for bioremediative technology of oxochlorate-contaminated water.



© 2008 International Union of Crystallography
 All rights reserved

Here, we report the overexpression, purification, crystallization and preliminary X-ray analysis of Cld from *A. oryzae* strain GR-1.

2. Experimental procedures

2.1. Selection of the *cld* gene for overexpression

A. oryzae strain GR-1, previously known as bacterial strain GR-1, was grown on chlorate-containing medium and the native chlorite dismutase was purified as described previously (Hagedoorn *et al.*, 2002).

The N-terminal amino-acid sequence was determined by selecting the 30 kDa band corresponding to the purified native Cld monomer from a 15% SDS-PAGE gel. This sample was subjected to 11 cycles of Edman (phenylisothiocyanate) degradation (Eurosequence, the Netherlands).

The resulting sequence (M/S)QPMQ(P/A)MKIER was reverse-translated and used to design degenerate forward primers. However, it also became clear that the *A. oryzae* Cld N-terminus is nearly identical to the 11 N-terminal amino acids of *Dechloromonas aromatica* Cld (MQPMQSMKIER). The backward degenerate primer was therefore based on the DNA sequence corresponding to the C-terminus of *D. aromatica* Cld. Combination of these primers yielded a 747 base-pair product in a PCR reaction with *Azospira* whole cells. The fragment was purified on an agarose gel and sequenced (Baseclear, the Netherlands).

Although the gene amplified by PCR was now available, generating the restriction sites and insertion into the plasmid was unsuccessful. Owing to these practical problems, the *cld* gene was chemically synthesized and cloned into pET28a using *Nde*I and *Bam*HI restriction sites, creating the vector pET28a-CDBC (Baseclear, the Netherlands) that includes an N-terminal His tag and a thrombin cleavage site. The resulting expressed protein from this plasmid carries 20 extra amino acids at the N-terminus (MGSSH-HHHHSSGLVPRGSH). The new construct was sequenced again, shown to be free of mutations or other errors and transformed into *Escherichia coli* BL21(DE3)pLysS cells.

2.2. Overexpression and purification of Cld

To produce haem-containing protein for crystallization and subsequent structural analysis, 10 ml cultures were grown overnight on a rotary shaker (220 rev min⁻¹) at 310 K. Erlenmeyer flasks with

500 ml LB medium including haemin (40 µg ml⁻¹), kanamycin (50 µg ml⁻¹) and chloramphenicol (25 µg ml⁻¹) were inoculated 1:50 from these overnight cultures. Growth was continued under the same conditions until the absorbance at 600 nm reached a value of 0.5. The temperature of the incubator was lowered to 303 K and 1 mM IPTG was added. Cultures were left to grow overnight (approximately 16 h) and cells were harvested by centrifugation at 277 K. Pellets were frozen immediately for storage prior to purification.

To purify Cld, the cell paste from 0.5 l culture was resuspended in 10 ml buffer A (20 mM Tris-HCl buffer pH 7.5, 500 mM NaCl) with 50 mM imidazole. Benzonase (50 units; Sigma-Aldrich) was added to reduce the viscosity owing to released DNA and cells were disrupted by sonication on ice. The lysate was centrifuged and loaded onto a 5 ml HisTrap FF crude column. The column was washed with five column volumes of 20 mM Tris-HCl buffer pH 7.5, 500 mM NaCl and 50 mM imidazole and the bound protein was directly eluted with 20 mM Tris-HCl buffer pH 7.5, 500 mM NaCl and 500 mM imidazole. After a step elution with five column volumes of buffer A supplemented with 500 mM imidazole, the Cld was desalted on a HiPrep 26/10 column equilibrated with 20 mM Tris-HCl pH 7.5. Subsequently, Cld was bound to a Resource-S cation-exchange column, washed with low ionic strength desalting buffer and eluted with a gradient of 0–1 M NaCl in 20 mM Tris-HCl pH 7.5. A highly concentrated dark-red fraction corresponding to active Cld eluted at approximately 135 mM NaCl. This solution was loaded onto a HiLoad 16/60 Superdex 200 prep-grade column equilibrated with 20 mM Tris-HCl pH 7.5, 135 mM NaCl. At a low flow rate (0.3 ml min⁻¹) the red-coloured tetrameric species was separated from a small amount of colourless monomeric Cld. All columns were obtained from Amersham Biosciences (Sweden) and mounted on an ÄKTAexpress protein-purification system (GE Healthcare) and all purification steps were performed at 277 K. The haem-containing Cld fractions of the gel-filtration step were combined and concentrated to 75 mg ml⁻¹ using an Amicon concentrator. The purified Cld was stored in 20 mM Tris-HCl pH 7.5, 135 mM NaCl at 193 K until further use.

To assay the activity of the monomeric and tetrameric Cld, 1 µl sample (15 mg ml⁻¹) was mixed with an equal volume of a 15 mM ClO₂⁻ solution and observed through a microscope. When tetrameric Cld was used gas bubbles evolved immediately upon mixture of the droplets, indicating that the tetrameric Cld used in the crystallization experiments is in the active form.

2.3. Crystallization and data collection

Prior to crystallization, the protein sample was filtered through a 0.22 µm low-binding protein filter (Millipore) to remove dust particles and protein precipitate. Crystallization attempts were made using various commercially available screens. Thin needle-shaped crystals were observed in JCSG+ screen (Qiagen) condition No. 81: 0.1 M potassium thiocyanate and 30% (w/v) PEG MME 2000. This condition was optimized on Q-plates using sitting-drop vapour diffusion at 295 K and a grid with 0–1.0 M potassium thiocyanate, 0–35% (w/v) PEG MME 2000 in a pH range from 3.6 to 9.0 using different buffers. 1 µl protein solution (6 mg ml⁻¹ in 20 mM Tris-HCl pH 7.5, 135 mM NaCl) and 1 µl reservoir solution were mixed and equilibrated against 750 µl of the same reservoir solution. Very thin rectangular plate-shaped crystals appeared in 100 mM MES buffer pH 5.5, 25% (w/v) PEG MME 2000, 0.3 M KSCN. This condition was further optimized using Additive Screen (Hampton Research). Hence, 1 µl protein solution (6 mg ml⁻¹ in 20 mM Tris-HCl pH 7.5, 135 mM NaCl) and 1 µl reservoir solution [100 mM MES buffer pH 5.5,

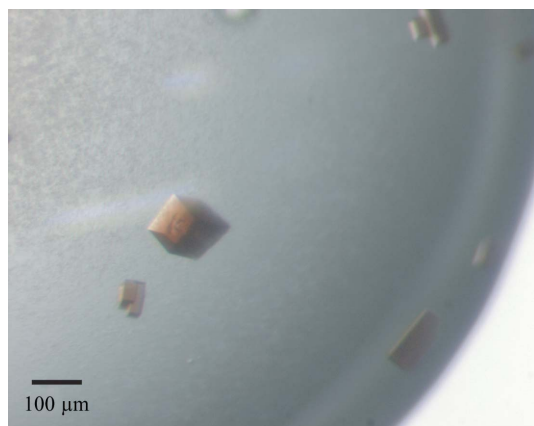


Figure 1
Crystals of Cld grown in 0.1 M MES pH 5.5, 25% (w/v) PEG MME 2000, 0.3 M KSCN, 5% glycerol and 180 mM ammonium sulfate. Maximum dimensions were reached after 7–10 d.

Table 1

Data-collection and processing parameters for a single Cld crystal.

Data statistics for the outer resolution shell are given in parentheses where applicable.

	Peak	Inflection point	High-energy remote
Crystal dimensions (μm)	80 × 80 × 80	80 × 80 × 80	80 × 80 × 80
Temperature (K)	100	100	100
Crystal system	Orthorhombic	Orthorhombic	Orthorhombic
Space group	$P2_12_12$	$P2_12_12$	$P2_12_12$
Unit-cell parameters (\AA)	$a = 164.71, b = 169.55,$ $c = 60.85$	$a = 165.00, b = 169.80,$ $c = 60.92$	$a = 164.46, b = 169.34,$ $c = 60.79$
Wavelength (\AA)	1.7382	1.7399	0.98340
Resolution range (\AA)	50–2.7 (2.85–2.70)	50–2.9 (3.06–2.90)	40.13–2.1 (2.21–2.1)
Reflections	660269 (96695)	538131 (78769)	731403 (107833)
Unique reflections	47838 (6864)	38886 (5579)	100003 (14403)
Redundancy	13.8 (14.1)	13.8 (14.1)	7.3 (7.5)
R_{merge}^\dagger (%)	10.7 (41.0)	10.9 (42.0)	10.5 (48.8)
Completeness (%)	100 (100)	100 (100)	100 (100)
Mean $I/\sigma(I)$	25.1 (6.3)	25.3 (6.1)	15.8 (3.8)
R_{anom}^\ddagger (%)	3.8 (10.9)	3.4 (10.9)	4.3 (19.3)
Anomalous multiplicity	7.2 (7.2)	7.3 (7.3)	3.7 (3.7)
Anomalous completeness (%)	100 (100)	100 (100)	100 (100)

$^\dagger R_{\text{merge}} = \sum_{hkl} \sum_i |I_i(hkl) - \langle I(hkl) \rangle| / \sum_{hkl} \sum_i I_i(hkl)$, where $I_i(hkl)$ is the intensity of the i th measurement of the same reflection and $\langle I(hkl) \rangle$ is the mean observed intensity for that reflection. $^\ddagger R_{\text{anom}} = \sum_h |I_{hi} - I_{-hi}| / \sum_h (I_{hi})$, where I_{hi} and I_{-hi} are Friedel pairs.

25% (w/v) PEG MME 2000, 0.3 M KSCN] were mixed with 0.2 μl additive solution. A condition with 0.1 M $(\text{NH}_4)_2\text{SO}_4$ as the additive resulted in larger crystals. Finally, the $(\text{NH}_4)_2\text{SO}_4$ concentration was varied between 0.05 and 0.3 M with or without the addition of 5% (v/v) glycerol. Triangular plates, cubic and bipyramidal crystals of up to approximately 100 × 100 × 100 μm in size were grown from well solutions containing 100 mM MES buffer pH 5.5, 25% (w/v) PEG MME 2000, 0.3 M KSCN, 5% (v/v) glycerol and 160–260 mM $(\text{NH}_4)_2\text{SO}_4$. An example of a cubic shaped Cld crystal is shown in Fig. 1. The two other crystal shapes were also tested but appeared to be of lower diffraction quality. The data were not sufficient to determine whether all these crystal shapes belonged to the same space group.

Prior to data collection at cryogenic temperatures, crystals were soaked in a solution containing the mother liquor including 16% glycerol and flash-frozen in a stream of nitrogen gas at 100 K using an Oxford Cryosystems Cryostream device. Multiple-wavelength anomalous dispersion (MAD) data were collected using an ADSC Quantum Q315r detector on beamline ID23-1 at the ESRF, Grenoble, France. Three wavelengths were chosen near the iron-absorption edge based on an X-ray fluorescence scan of the frozen crystal. The f'' component (peak) and the $\Delta f'$ (remote) were maximized, while the f' component (inflection point) was minimized. Data were collected with a 1° rotation and 0.2 s exposure time per frame. The intensities were indexed with *MOSFLM* (Leslie, 1999) and scaled using *SCALA* (Evans, 2006) from the *CCP4* program suite (Collaborative Computational Project, Number 4, 1994).

The refined unit-cell parameters are $a = 164.46$, $b = 169.34$, $c = 60.79$ \AA and analysis of the X-ray diffraction pattern showed that reflections along the h and k axes were only present if $h, k = 2n$, identifying the space group as $P2_12_12$. A Matthews coefficient (Matthews, 1968) of 2.54 $\text{\AA}^3 \text{Da}^{-1}$ suggested the presence of six

subunits of 28 kDa in the asymmetric unit, corresponding to 51.6% solvent content. Data-collection statistics are given in Table 1. The six iron sites could be identified, phases could be obtained and model building is in progress. The phasing and the structure determination will be published in detail elsewhere.

The authors would like to thank Dr Nora Goossen and Dr Ir Peter-Leon Hagedoorn for initial discussions on this project, Igor Nederlof for help with the setup of the initial screens and Dr Ir Bert Jansen for data collection. We acknowledge the European Synchrotron Radiation Facility for provision of synchrotron-radiation facilities and we would like to thank Dr David Flot for assistance in using beamline ID23-1.

References

- Collaborative Computational Project, Number 4 (1994). *Acta Cryst.* **D50**, 760–763.
- Evans, P. (2006). *Acta Cryst.* **D62**, 72–82.
- Ginkel, C. G. van, Rikken, G. B., Kroon, A. G. & Kengen, S. W. (1996). *Arch. Microbiol.* **166**, 321–326.
- Hagedoorn, P. L., de Geus, D. C. & Hagen, W. R. (2002). *Eur. J. Biochem.* **269**, 4905–4911.
- Hou, S., Larsen, R. W., Boudko, D., Riley, C. W., Karatan, E., Zimmer, M., Ordal, G. W. & Alam, M. (2000). *Nature (London)*, **403**, 540–544.
- Kengen, S. W., Rikken, G. B., Hagen, W. R., van Ginkel, C. G. & Stams, A. J. (1999). *J. Bacteriol.* **181**, 6706–6711.
- Leslie, A. G. W. (1999). *Acta Cryst.* **D55**, 1696–1702.
- Matthews, B. W. (1968). *J. Mol. Biol.* **33**, 491–497.
- Rikken, G. B., Kroon, A. G. M. & van Ginkel, C. G. (1996). *Appl. Microbiol. Biotechnol.* **45**, 420–426.
- Wilson, M. T. & Reeder, B. J. (2008). *Exp. Physiol.* **93**, 128–132.
- Wolterink, A., Kim, S., Muusse, M., Kim, I. S., Roholl, P. J., van Ginkel, C. G., Stams, A. J. & Kengen, S. W. (2005). *Int. J. Syst. Evol. Microbiol.* **55**, 2063–2068.